Electronic Supplementary Material (ESI) for Physical Chemistry Chemical Physics
This journal is © The Owner Societies 2013

Supporting information for:

Introducing a standard method for experimental determination of the solvent response in laser pump, x-ray probe time-resolved wide-angle x-ray scattering experiments on systems in solution

Kasper Skov Kjær,[a] Tim B. van Driel,[b] Jan Kehres,[b] Kristoffer Haldrup,[b] Dmitry Khakhulin,[c] Klaus Bechgaard,[d] Marco Cammarata,[e] Michael Wulff,*[c] Thomas Just Sørensen*[d] and Martin M. Nielsen*[b]

Contents

Electronic Supplementary Material (ESI) for Physical Chemistry Chemical Physics
This journal is © The Owner Societies 2013

1. Absorption spectra

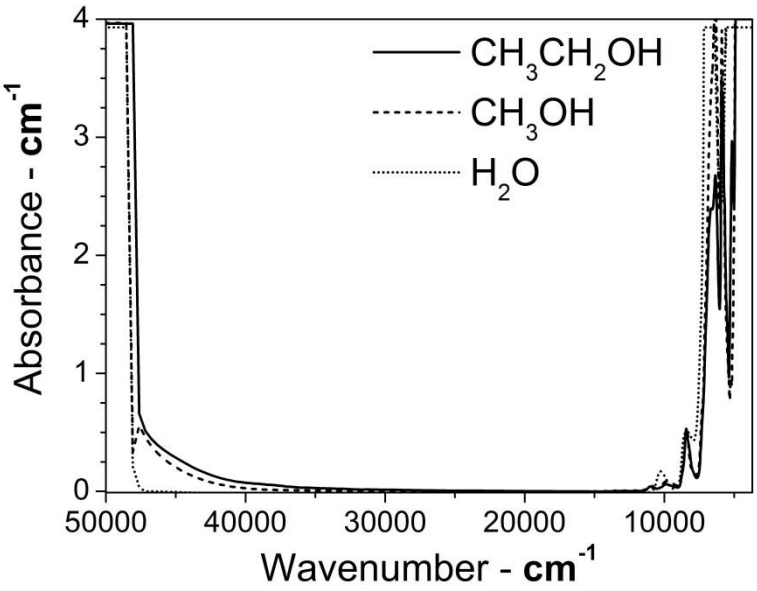

Figure S1. Absorption spectra of alcohols.

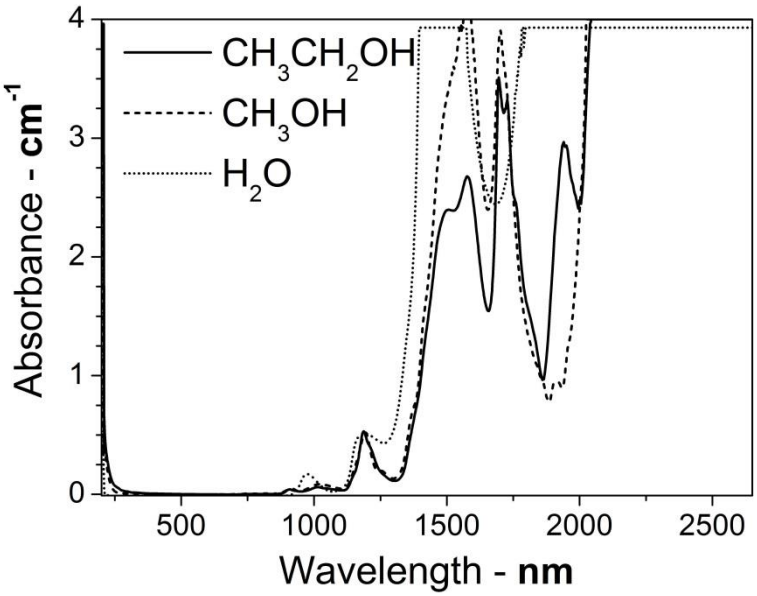

Figure S2. Absorption spectra of alcohols.

Electronic Supplementary Material (ESI) for Physical Chemistry Chemical Physics
This journal is © The Owner Societies 2013

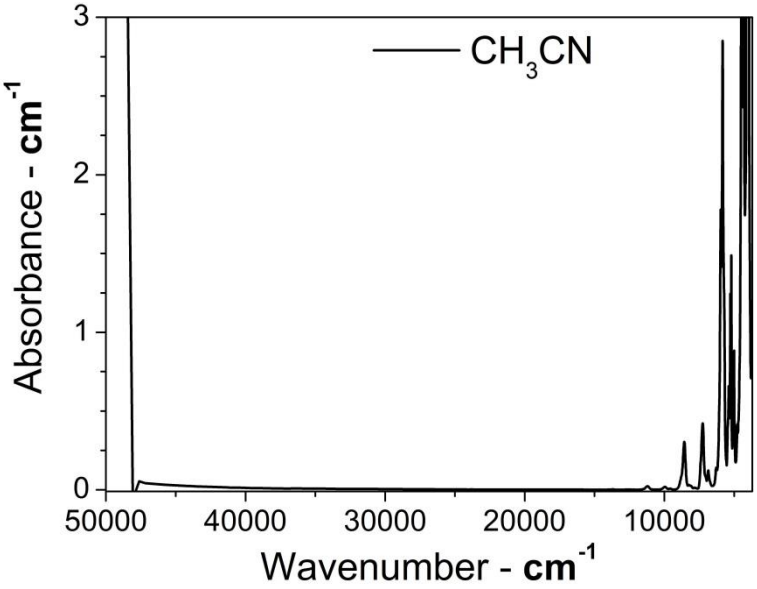

Figure S3. Absorption spectrum of acetonitrile.

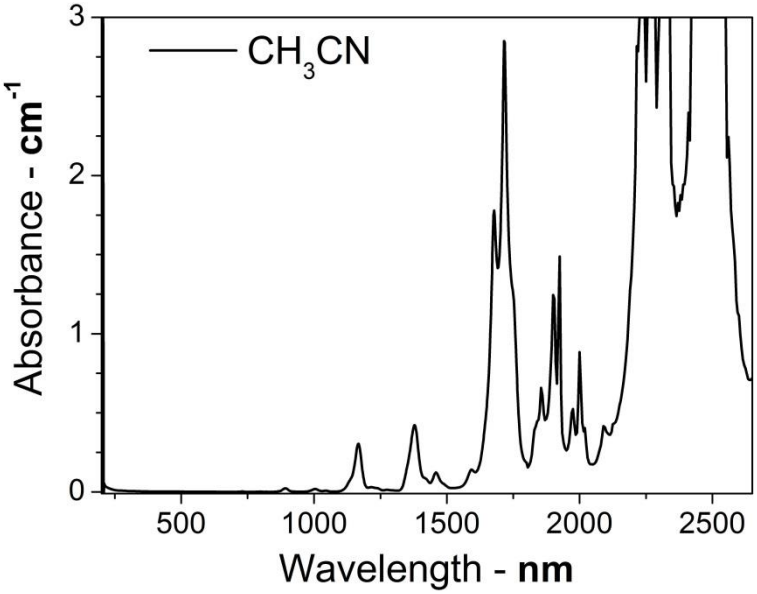

Figure S4. Absorption spectrum of acetonitrile.

Electronic Supplementary Material (ESI) for Physical Chemistry Chemical Physics
This journal is © The Owner Societies 2013

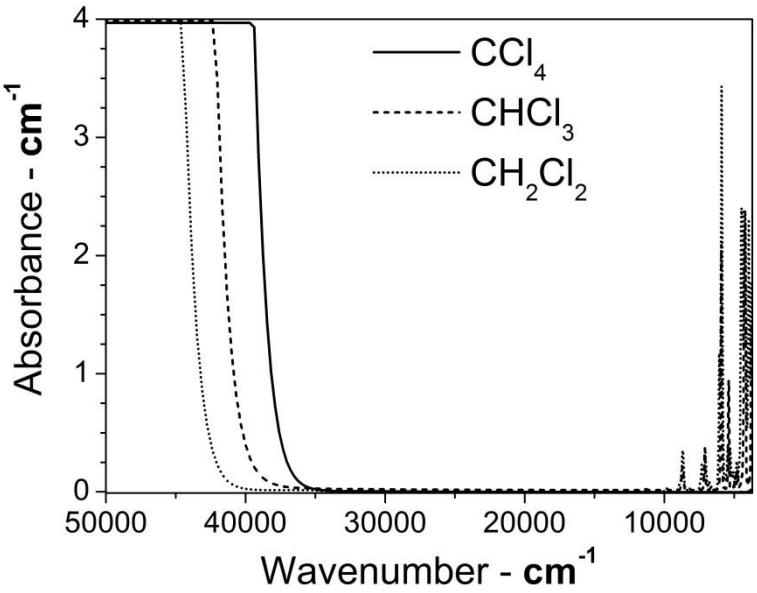

Figure S5. Absorption spectra of chlorinated solvents.

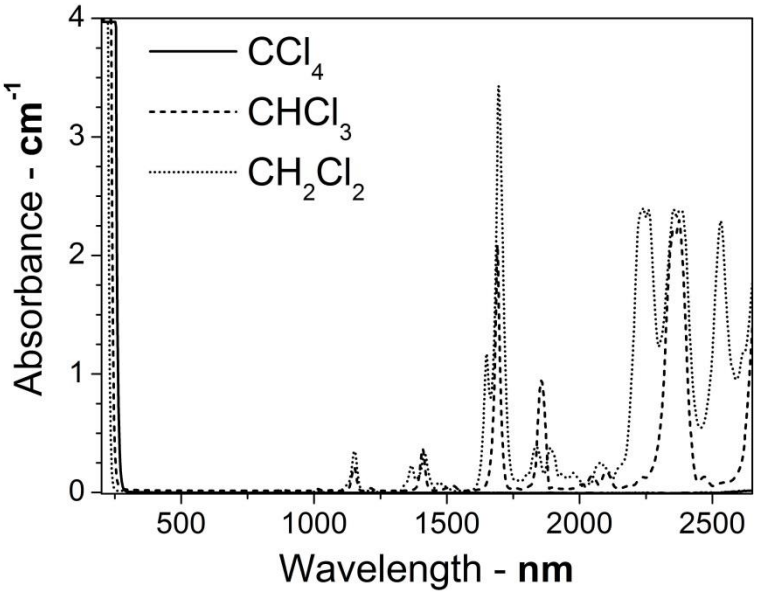

Figure S6. Absorption spectra of chlorinated solvents.

Electronic Supplementary Material (ESI) for Physical Chemistry Chemical Physics
This journal is © The Owner Societies 2013

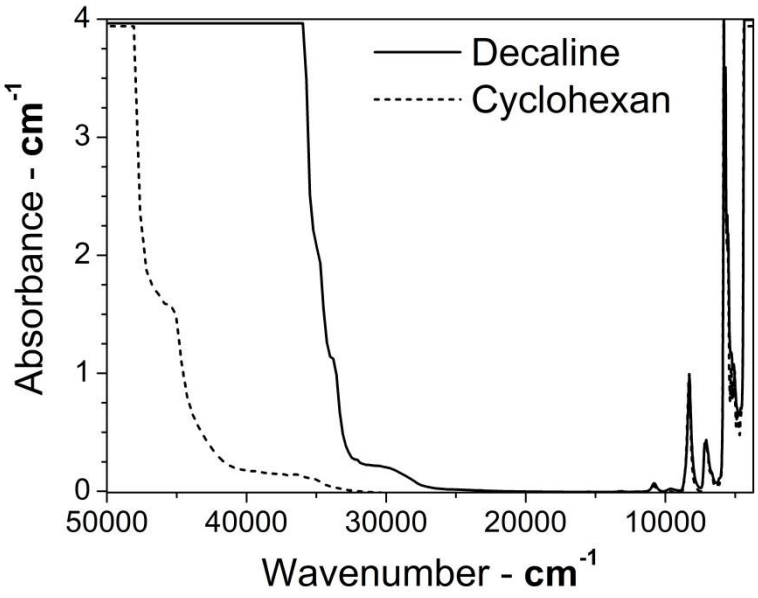

Figure S7. Absorption spectra of alkanes.

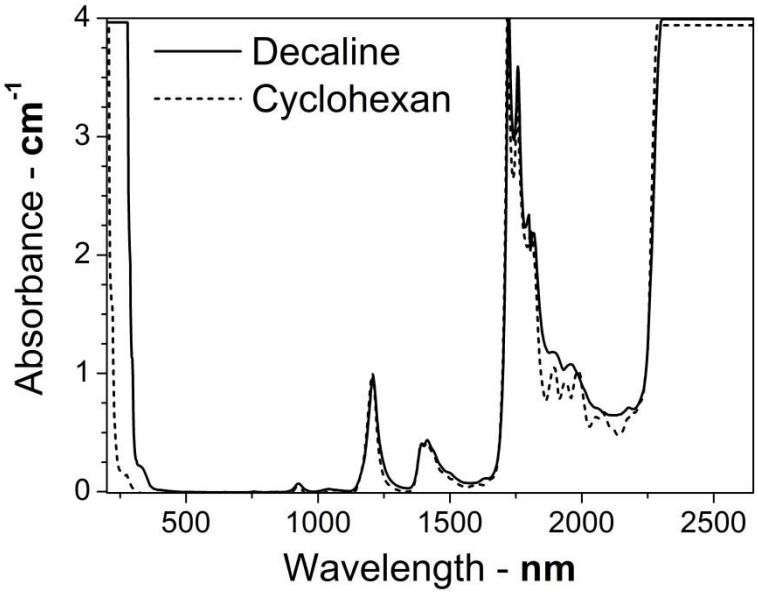

Figure S8. Absorption spectra of alkanes.

Electronic Supplementary Material (ESI) for Physical Chemistry Chemical Physics
This journal is © The Owner Societies 2013

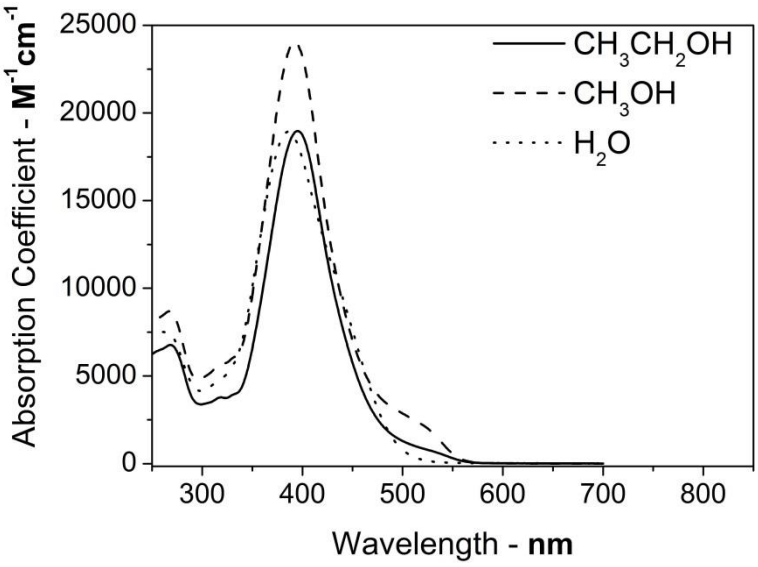

Figure S9. Absorption spectra of Fast Yellow (**1**, sodium 4-aminoazobenzene-3,4'-disulphonate, CAS 2706-28-7) at high dilution in various solvents.

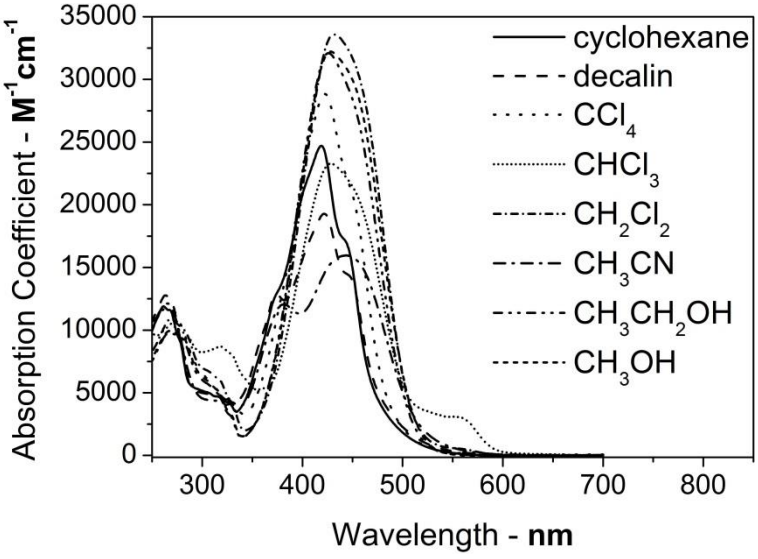

Figure S10. Absorption spectra of 4-bromo-4'-(N,N-diethylamino)-azobenzene (**2**, CAS 22700-62-5)) at high dilution in various solvents.

Electronic Supplementary Material (ESI) for Physical Chemistry Chemical Physics
This journal is © The Owner Societies 2013

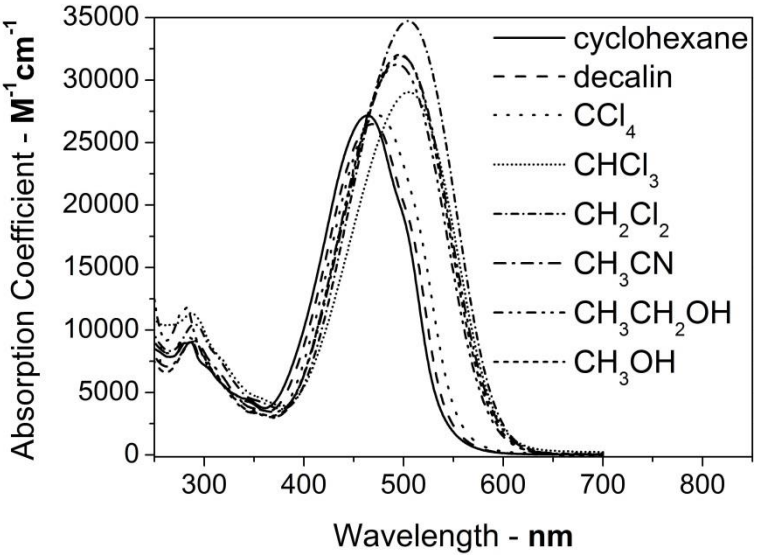

Figure S11. Absorption spectra of 4-(N,N-diethylamino)-2-methoxy-4'-nitro-azobenzene (**3**, CAS 6373-95-1) at high dilution in various solvents.

Electronic Supplementary Material (ESI) for Physical Chemistry Chemical Physics
This journal is © The Owner Societies 2013

2. Data processing – from raw data to difference scattering curves

The 2D detector images were first corrected for the (small) spatial distortion from the taper optics in the Frelon CCD. Then the dark current signal was subtracted and the sensitivity of each pixel uniformity corrected. After these corrections the full 2D images were corrected for the polarization of the x-ray beam, the x-ray absorption in the liquid sheet, the incidence angle of each detector pixel and the absorption of the x-rays in the phosphor screen of the detector. The final correction is the subtraction of air scattering.
This was followed by azimuthal integration resulting in the data-sets shown in FigureS12.

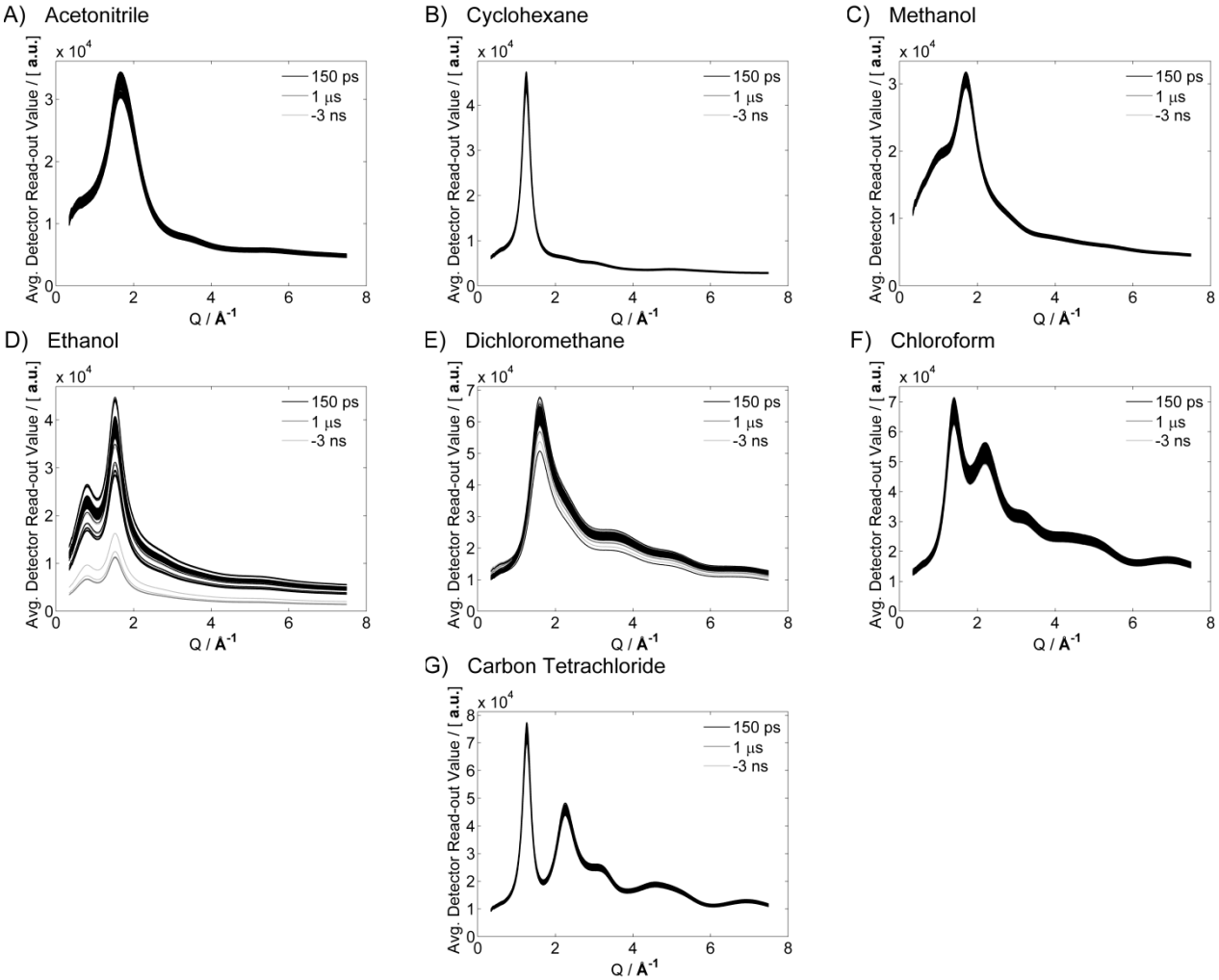

Figure S12. Raw data: Azimuthally integrated detector readout valies, each panel shows 600 individual scattering curves recorded at three different time-delays.

Electronic Supplementary Material (ESI) for Physical Chemistry Chemical Physics
This journal is © The Owner Societies 2013

At high Q the solvent scattering has little contribution from intermolecular structure. The high-Q range can therefore be used to normalize the scattering curves to the simulated scattering of the constituent atoms of the solvent molecules taken independently.
The simulated scattering used to normalize the signals was calculated as the sum of the atomic form factors and the incoherent scattering of the constituent atoms of a single solvent molecule. The atomic form factors were calculated from the Cromer-Mann parameterization. The incoherent scattering was calculated using the numerical approximation introduced by Hajdu [F. Hajdu, Acta Crystallogr., 1972, A28, 250-252].
Thus, for e.g. acetonitrile the incoherent scattering and form factors were calculated for a nitrogen atom, three hydrogen atoms and two carbon atoms and used to normalize the data.
Some care has to be taken for the chlorinated solvents (see figure S13), where the signal in the high-Q range still has a significant modulations arising from well-defined distances between the strongly scattering Cl atoms.

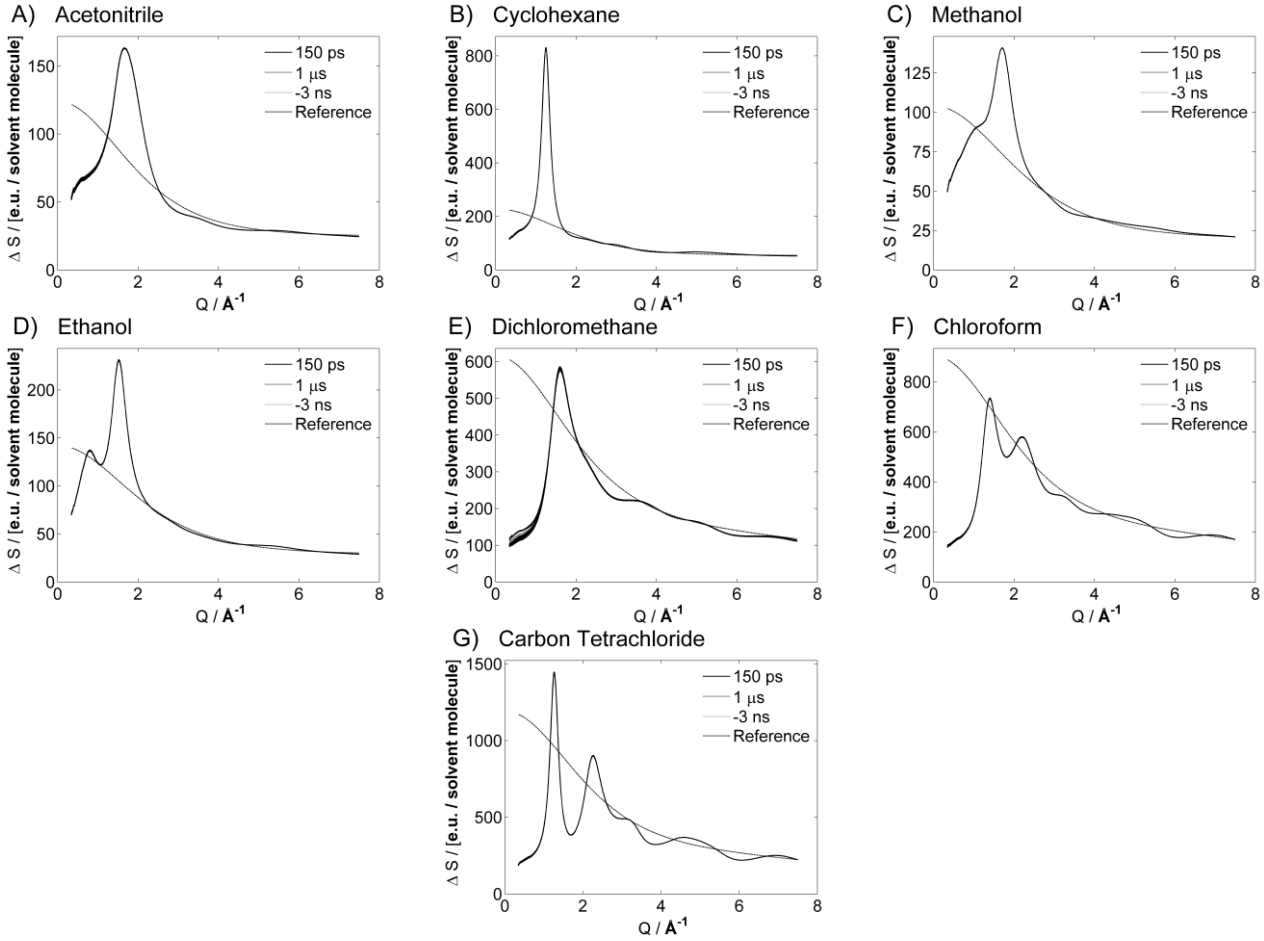

Figure S13. Normalised scattering curves: radially integrated detector readout normalized at high Q to gas phase scattering. The scattering curves are normalised to the scattering of a single solvent molecules, the raw data is divided by the simulated scattering of a single solvent molecule in atomic units. The panels show the resulting normalised scattering curves (solid lines, 600 curves) and the simulated 'gas phase scattering' of a single solvent molecule (dashed line).

Electronic Supplementary Material (ESI) for Physical Chemistry Chemical Physics
This journal is © The Owner Societies 2013

Following normalization, the difference scattering intensities ΔS were generated from the scattering curves recorded at a positive time delay by subtracting the average of the two nearest scattering curves recorded at a negative time delay. Difference curves from the same pump-probe time-delay (Δt) were summed after an outlier rejection based on a point-by-point implementation of Chauvenet's criterion.

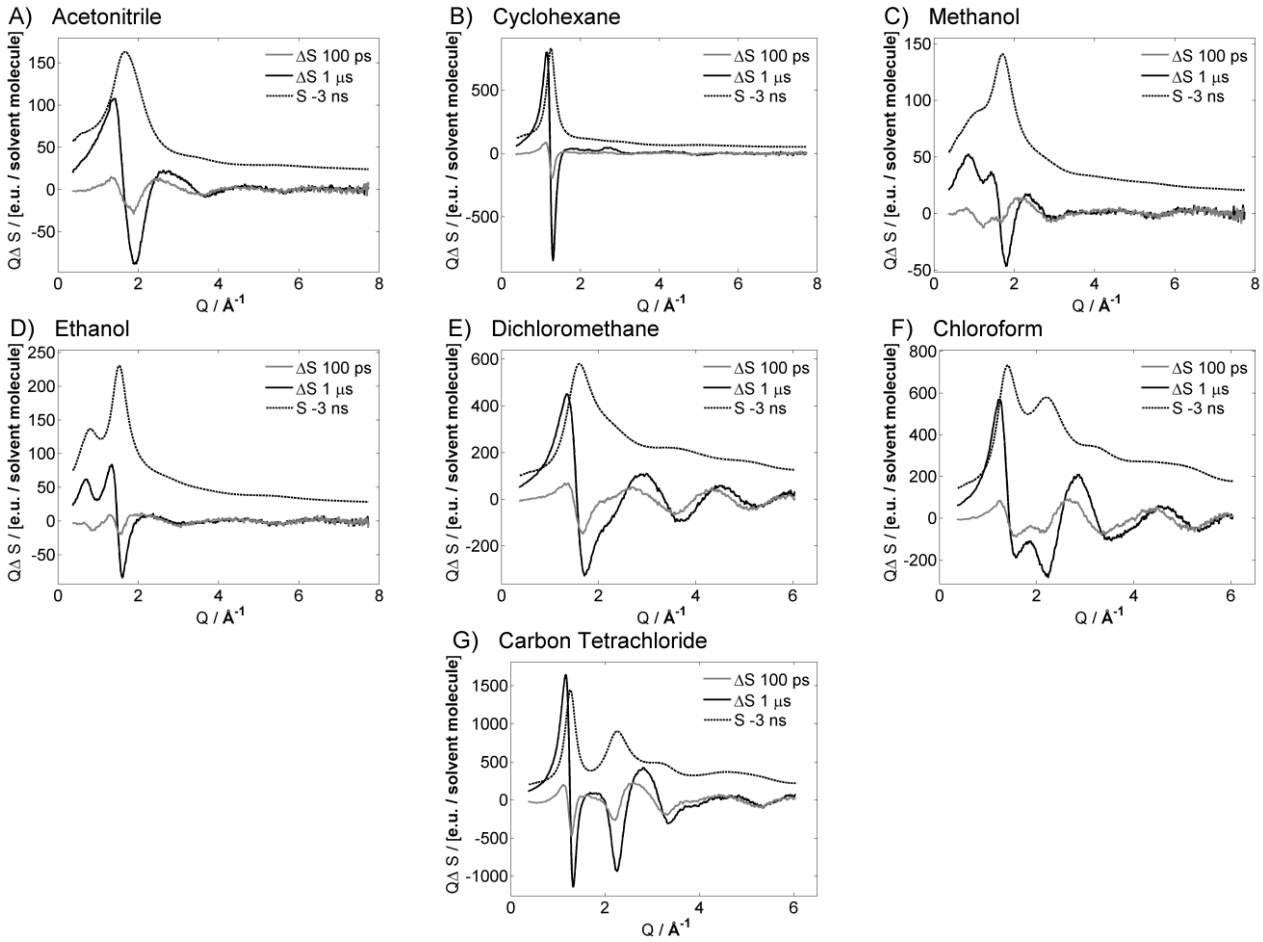

Figure S14. Difference scattering curves (x500) with total scattering signal: The difference scattering curves obtained by subtracting scattering curve from the negative time delay from the scattering curve of the positive time delay. The scattering curve is shown to illustrate which peaks that change at the two delay times.

Electronic Supplementary Material (ESI) for Physical Chemistry Chemical Physics
This journal is © The Owner Societies 2013

The difference scattering curves recorded for the 100 ps and 1 µs time-delay were used to derive the solvent differentials shown in figure 5 of the main text in the following way:

1) The temperature-change at the 1 µs time-delay was determined by comparing ΔS(1µs) to the differences between steady-state scattering curves recorded at 20, 25 and 30°C.

$$\Delta T(1\mu s) = 10°C \cdot \left(\frac{\Delta S(1\mu s)}{S(30°C) - S(25°C)} + \frac{\Delta S(1\mu s)}{S(25°C) - S(20°C)}\right)$$

2) The temperature-change after 100ps, ΔT(100ps) was determined through eq. 7 in the main text. This allowed for determining the temperature differential from eq. 5 of the main text:

$$\left.\frac{\partial \Delta S}{\partial T}\right|_{\rho} = \frac{\Delta S(100\ ps)}{\Delta T(100\ ps)}$$

2) The remaining heat contribution to the signal after the thermal expansion is given by $\frac{C_V}{C_P}\Delta S(100\ ps)$. This was subtracted from the total difference scattering signal recorded at the 1 µs time delay. The resulting curve was scaled to the derived density change after 1µs as described by eq. 6 of the main text the density differential can be determined as:

$$\left.\frac{\partial \Delta S}{\partial \rho}\right|_{T} = \frac{\Delta S(1\ \mu s) - \frac{C_V}{C_P}\Delta S(100\ ps)}{\Delta \rho(1\ \mu s)}$$

The determined value for ΔT(100 ps), ΔT(1 µs) and Δρ(1 µs) are reported in table 4 of the main text.

Having determined the solvent differntials, we determined the noise of the obtained data as described by Haldrup et al. [K. Haldrup et al. *Acta Cryst. A*, 2010, **66**, 261-269.]. For each data-point a 2nd order polynomial is fitted to the interval of the 20 closest data-points. The standard-deviation (σ) for each data-point was then determined as the standard deviation between the fit and the data. Figure S15 shows the obtained solvent differentials and an envelope of ±1σ

Electronic Supplementary Material (ESI) for Physical Chemistry Chemical Physics
This journal is © The Owner Societies 2013

Figure 5 – establishing the area of confidence (estimation of uncertainty)

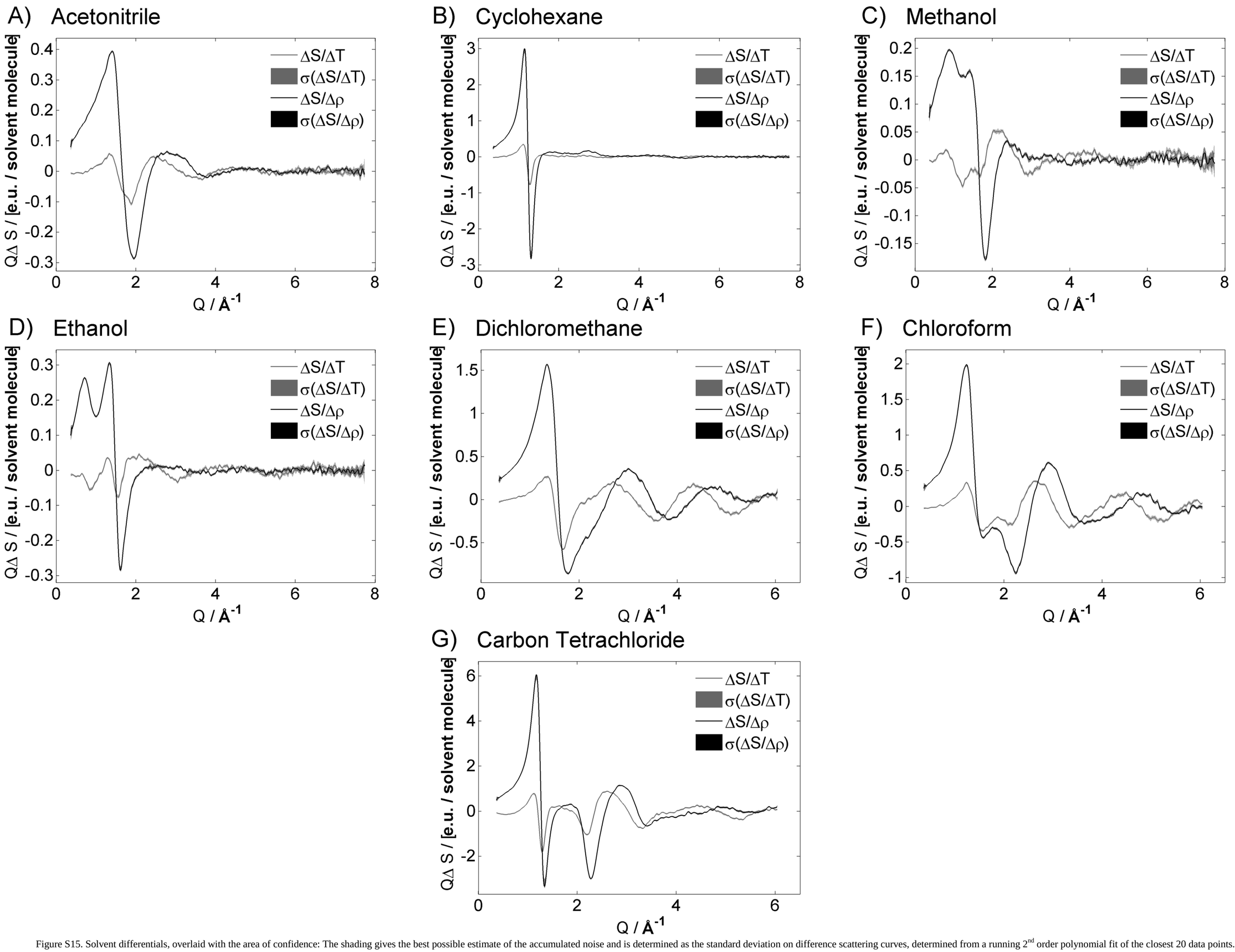

Figure S15. Solvent differentials, overlaid with the area of confidence: The shading gives the best possible estimate of the accumulated noise and is determined as the standard deviation on difference scattering curves, determined from a running 2nd order polynomial fit of the closest 20 data points.

Electronic Supplementary Material (ESI) for Physical Chemistry Chemical Physics
This journal is © The Owner Societies 2013

3. Point heating – energy dissipation from solutes

The energy pathway resulting from photoexciting a solute in solution is given in the main text as:

$$S_0 \xrightarrow{h\nu} S_n^* \xrightarrow{IC+IVR} S_1^* \xrightarrow{VR} S_1 \xrightarrow{IC} S_0^* \xrightarrow{VR} S_0$$

The energy absorbed in the solute will after a given time, typically accounted as five times the lifetime of the excited state, be fully deposited in the solvent. This amounts to a heating of the solvent, where each solute constitutes a source from where the solvent is heated. Considering nanoparticles or single molecules as solutes, these can be construed as point sources of heat deposition, when propagating the heat distribution within a classical framework.

Photoexciting a solute that exclusively releases energy to the solvent will give a result identical to a point heating event, where the solvent is heated by point-like heat sources randomly distributed in the solvent. Thus, the heat propagation of the experiment can be treated in the framework describing heat deposition from point sources distributed throughout the bath of solvent.

4. ΔT from optical density and temperature based measurements

The changes in temperature and density giving rise to the difference scattering curves of the late time-points (t >> L/v) can be found by scaling the difference scattering curves measured, to the difference between steady-state measurements recorded at different temperatures as described in section 2. However, the high degree of control of light absorption in the experiment using the dye molecules allows for direct estimates of the deposited energy from the experimental parameters. The direct calculation of the expected temperature increase from the amount of energy absorbed by dye molecules in the irradiated volume can be done as described here:
For a Gaussian laser pulse with FWHM d = 340μm, and energy E = 200 μJ, the peak fluency (E_0) is given by equation S1, where *l* is the liquid sheet thickness. Equation S2 transforms E_0 to the peak energy per volume E_v.

Eq. S1 $$E_0 = \frac{4 \cdot E \cdot \ln(2)}{(\pi d^2)} = 0.153 \text{ J·cm}^{-2}$$

Eq. S2 $$E_V = \frac{E_0}{l} = 5.09 \text{ J·cm}^{-3}$$

Assuming identical centers for the laser and x-ray spots, the average laser energy per volume in the x-ray exposed area (E_{sample}) for a circular laser pulse of diameter (FWHM) d_{laser} and a rectangular x-ray pulse of height (FWHM) $h_{x\text{-}ray}$ and width (FWHM) $w_{x\text{-}ray}$ is given by the ratio between the integral of the product of the pulse shapes and the integral of the x-ray pulse shape, with $c = \frac{1}{2\sqrt{2ln2}}$:

Electronic Supplementary Material (ESI) for Physical Chemistry Chemical Physics
This journal is © The Owner Societies 2013

Eq. S3
$$E_{\text{sample}} = E_V \frac{\int_{-\infty}^{\infty}\int_{-\infty}^{\infty} \exp\left(\frac{-x^2}{w_{x\text{-}ray}\cdot c}-\frac{y^2}{h_{x\text{-}ray}\cdot c}\right)\cdot\exp\left(\frac{-(x^2+y^2)}{d_{laser}\cdot c}\right)dxdy}{\int_{-\infty}^{\infty}\int_{-\infty}^{\infty} \exp\left(\frac{-x^2}{w_{x\text{-}ray}\cdot c}-\frac{y^2}{h_{x\text{-}ray}\cdot c}\right)dxdy}$$

$$= E_V \cdot \frac{\sqrt{\frac{1}{h_{x\text{-}ray}}}\sqrt{\frac{1}{w_{x\text{-}ray}}}}{\sqrt{\frac{d_{laser}+h_{x\text{-}ray}}{d_{laser}\cdot h_{x\text{-}ray}}}\sqrt{\frac{d_{laser}+w_{x\text{-}ray}}{d_{laser}\cdot w_{x\text{-}ray}}}} = 3.95\ \text{J}\cdot\text{cm}^{-3}$$

In most experiments, the sample had an absorptivity of 0.3 (an optical density of 0.15) and the reflectivity of the jet surface at normal incidence is given by $\left|\frac{1-n}{1+n}\right|^2$ (where *n* is the index of refraction, for acetonitrile the index of refraction is 1.346, which yields a reflectivity 0.022), the average deposited laser energy per volume (ΔE) probed by the X-rays becomes:

Eq. S4 $$\Delta E = E_{\text{sample}} \cdot 0.3 \cdot (1 - 0.022) = 1.18\ \text{J/cm}^3$$

The specific heat capacity at 25 °C of acetonitrile is C_P=1.763 J/cm^3·K, thus the average temperature change probed by the x-rays becomes:

Eq. S5 $$\Delta T = \frac{\Delta E}{C_P} = 0.61\ ℃$$

The largest error in calculating ΔT, will result from the determination of the optical density of the sample, for the experiments presented here the error is below 10 %.

Electronic Supplementary Material (ESI) for Physical Chemistry Chemical Physics
This journal is © The Owner Societies 2013

5. How to measure a solvent response - expanded

A solution of one of the three dyes should be prepared such that the optical density of the sample at the wavelength of the pump laser is around 0.6 (e.g. ~0.6 g/L of dye2, in a 300µm liquid sheet, at 400 nm). Absorption spectra of the three dyes in a range of solvents are shown in FigureS09 to Figure S11 in section 1 of the SI.

The laser peak fluency should be in the high end of the linear regime around 100-150 GW/cm^2 (0.2 J/cm^2 at 1.2 ps pulse length). For a typical 300 µm liquid sheet, the energy-deposition should amount to around 5 J/cm^3, and around 15 J/cm^3 for a 100 µm liquid sheet. These are 'typical' experimental values and should give standard signal to noise ratios.

In principle, only two time-delays are needed. One delay before the onset of the thermal expansion, and one after the thermal expansions has run to completion ($t << L/v$ and $t >> L/v$, as described in the main text). We have observed that the density response around ~2*L/v is slightly larger than that of the fully thermalized solution. Furthermore the limit of non-negligible contribution of the density differential sets in around 0.1*L/v. Usually, a delay in the 100 ps - 500 ps range, a delay in the 1 µs - 3 µs range and a reference delay should be used.

The early time-point will contain the signal from the temperature change caused by the energy deposition at constant volume ($\Delta T=\Delta E/C_v$). While the late time-point will contain the signal from the temperature and density change experienced by the probe pulse after the thermal expansion has run its course ($\Delta T=\Delta E/C_p$ $\Delta\rho= \alpha_v*\Delta E/C_p$).

Having chosen time-delays of e.g. 100ps and 1µs, the difference scattering curves – ΔS(100ps) and ΔS(1 µs) – can be generated from the data recorded at these two time-delays and the reference data as described in section 2 of the SI.

If there is no need for the absolute values of density and temperature change two unscaled solvent differentials can be generated directly from the two difference scattering curves. ΔS(100 ps) can act directly as an unscaled temperature differential, whereas ΔS(1 µs)-Cv/Cp*ΔS(100 ps) directly act as an unscaled density differential.

If there is a need for the absolute values of density and temperature change, the temperature change after the thermal expansion (here ΔT(1µs)), can be obtained from the late difference scattering signal (ΔS(1µs)). This can either be done through a set of steady-state measurements at different temperatures or by evaluating the deposited energy experienced by the x-ray probe pulse, as described in the end of section 2 and section 4 respectively. The temperature-change after the thermal expansion allows for absolute quantification of the temperature-change before the thermal expansion, and the density change after the thermal expansion, allowing for absolute scaling of the two solvent differentials as described in the end of section 2.

If NIR excitation is preferred, a wavelength should be chosen where the optical density of the sample is greater than 0.1 and the laser fluency should be adjusted to the optical density such that the initial temperature increase is no larger than 2 K. This will in most cases ensure that the data is recorded at a laser power lower that the breakdown of the linear response, although this might not be possible for all solvents (e.g. acetonitrile as shown in the main text).

Electronic Supplementary Material (ESI) for Physical Chemistry Chemical Physics
This journal is © The Owner Societies 2013

6. NIR excitation of acetonitrile

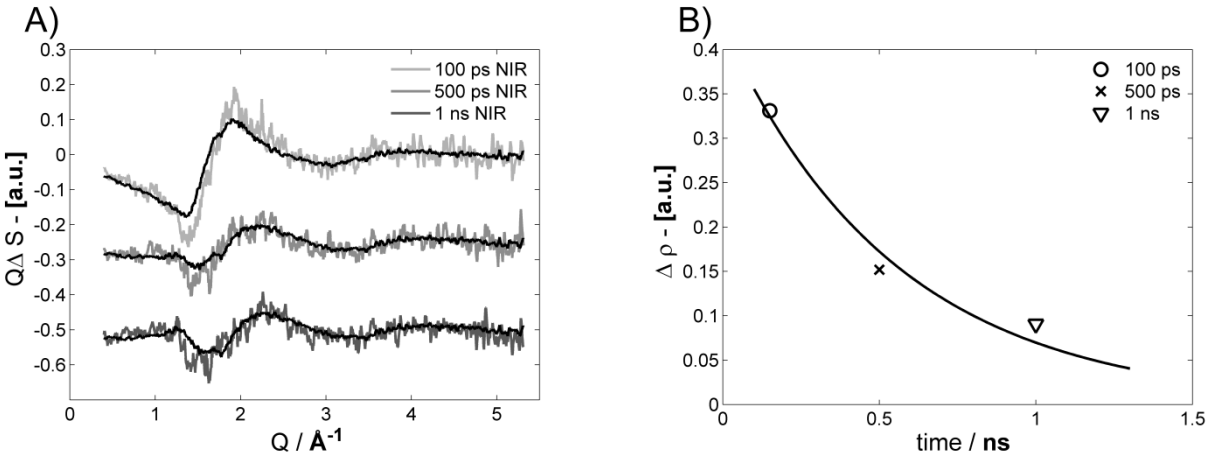

FigureS16. (A) Shows the difference scattering signal recorded at three timedelays after excitation of neat acetonitrile at 1718 nm. Black curves are fits using the solvent term derived for acetonitrile in the main text, allowing for quantification of Δρ and ΔT. (B) Shows the magnitude of Δρ determined for the three pump-probe delays. Black curve is an exponential fit with a life-time of 0.5 ns.

Difference scattering was recorded after excitation of neat acetonitrile at 1718 nm at 150ps, 500 ps, 1 ns and 1 µs time delays. Analysis of the data shows that the difference signal can be fitted well using the solvent differentials determined for acetonitrile allowing for quantification of Δρ and ΔT (fits shown in FigureS16(A)). The fitting procedure show a significant density increase is present at the 150 ps. The densitit increase decays with roughly a 0.5 ns time constant. The temperature change is constant throughout these early times. The 1 µs time-delay (not shown) is indistinguisable from acetonitrile having undergone pure point-heating.

Completely parallel behaviour of a short-lived density increase on the sub-nanosecond time-scale after a NIR pump event has been observed methanol at high pump fluencies [E. Pontecorvo, PhD thesis, UNIVERSITÁ DEGLI STUDI DI ROMA, 2006]. The methanol study was carried out at a large range of laser-fluencies, and the effect was only present above a fluency threshold of ~1 J/cm^2. The effect was ascribed to the formation of micro-bubbles in the first microns of the liquid sheet due to higher-order absorption processes leading to an extremely high local heat deposition in the front of the liquid sheet. Simmilar observations of very short-lived density increases have been found by Kotaidis et al., as well as ourselves, stemming from micro-cavitation of the solvent caused by flash-boiling from nanoparticle surfaces [unpublished results, V. Kotaidis, C. Dahmen, G. von Plessen, F. Springer and A. Plech, *J. Chem. Phys*, 2006, 124, 184702.].

Thus, we assign the short-lived deviation of the acetonitrile signal recorded after NIR excitation from that of the expected evolution of the hydrodynamic parameters to short-lived micro-bubble formation. The fluency-threshold of the onset of the micro-cavitation for NIR excitation of acetonitrile is much lower than for methanol. This entails that no fluencies where a detectable difference signal can be observed for acetonitrile, can the early time-points of the data be fitted without including a positive density term

This means that it is impossible to identify a set of experimental parameters that allows for extraction of the solvent differentials of acetonitrile using NIR mediated energy deposition.

Electronic Supplementary Material (ESI) for Physical Chemistry Chemical Physics
This journal is © The Owner Societies 2013

7. Description of the experimental protocol

The details of the setup can be found in Appendix B and section 2.2 of the main text.

An amount of Dye 2 was dissolved in each solvent such that the OD of the 300 µm liquid sheet was 0.15 (resulting in a 0.3fraction of the incident pump photons being absorbed in the sample). The sample reservoir was kept at 25°C in a thermal bath. Scattering curves were recorded at Δt = -3ns, 100ps, 1 µs pump-probe time delay. The series was repeated 200 times for each sample.

The concentration used for each of the dyes was lower than we would propose to use today (for an experiment conducted using 400 nm excitation with a 300 µm liquid sheet). The difference of the suggested concentration from the experiments we conducted is based on the results of the investigation of the linearity of the solvent response with the absorptivity of the sample (Panel A of figure 6). Here it was found that the response is linear up to an absorptivity of around 0.8 (0.6 OD).

Concentrations used in this study

Solvent	Concentration mg/l
MeCN	152
Cyclohexane	88
MeOH	86
EtOH	85
CH_2Cl_2	103
$CHCl_3$	80
CCl_4	85

Concentrations suggested for further studies

Solvent	Concentration mg/l
MeCN	607
Cyclohexane	352
MeOH	345
EtOH	338
CH_2Cl_2	313
$CHCl_3$	319
CCl_4	340

For the steady-state measurements at constant temperature, the scattering signal of each sample was measured at 20°C, 25°C and 30°C. The samples were given at least 1 hour to thermalize in a thermal bath kept at the temperature under investigation before the start of the measurement. To certify the sample temperature, it was measured with an external thermometer before the start of the measurement.